Proceedings of the 1. Conference on
Applied Mathematics and Computation
Dubrovnik, Croatia, September 13–18, 1999
pp. 223–232

Some Numerical Models of Fabric Structures

Krešimir Fresl*

Abstract. Form finding as the first phase of design of fabric structures is considered, with a minimal surface as a plausible mathematical model. Analysis is restricted to structures with fixed edges. A comparison is made of the two discretizations of the differential equation of minimal surface and the pertaining functional, namely, the finite difference and the finite element discretizations. Resulting system of nonlinear algebraic equations is solved by a variant of the full multilevel method with full approximation storage scheme. Numerical studies confirm that the multilevel method can be used as a robust and a stable solver with a fast convergence for both types of discretizations.

AMS subject classification: 74–04, 74G65, 74K15, 49Q05, 65N55

Key words: fabric structure, form finding, minimal surface, multigrid method

1. Introduction: on tensile fabric structures

Tentatively, we can define fabric structures as building structures that are primarily used for enclosure of large spaces, particularly those with wide spans clear between supports, and whose basic building material is (structural) fabric, acting as a membrane. Fabric is thus used both as a load bearing structure and as an enclosure [1].

Conventional massive and rigid structures can, by means of internal distribution of stresses, resist different kinds of stresses: tension, compression, shear. Stress distributions lead to complex stress patterns that can be observed in photoelastic experiments. Flexible ropes and fabric, on the other hand, can transmit only tension. They are, however, very efficient since they carry applied load by direct route, along their center line or middle surface, while the distribution of tensile stress is uniform (and they cannot "avoid" carrying load by buckling, as compressive members do).

Single rope or flimsy membrane will noticeably alter its shape when load changes its position or direction. Other means are therefore needed to give stability and stiffness to a structural system which is made up of flexible components or material. Cables must be arranged in a net; in a simple case there are two orthogonal families of cables: load bearing, concave cables in one direction, and stabilizing, convex cables in another. Similarly, fabric membrane must form an anticlastic surface. At the same time, cables and fabric must be subjected to a particular pattern of prestress, since tension should

*Faculty of Civil Engineering, University of Zagreb, Kačićeva 26, 10000 Zagreb, Croatia, e–mail: fresl@grad.hr

be retained even under unfavorable combinations of external loads. Anticlastic shape and, specially, prestress give so-called geometric stiffness to the tensile structure.

Thus, the form of a tensile fabric structure is critical to its structural behaviour. And conversely, structural laws of equilibrium govern the form: geometric form directly reflects the complex field of surface forces in equilibrium. Arbitrary geometric shapes cannot satisfy equilibrium conditions. There is a kind of a paradox: seemingly free, organic forms of tensile structures, "roofscapes", are in fact determined by strict physical laws.

Under the laws of equilibrium, the form of the tensile structure originates from the shape of the supporting structure: boundary beams, arches or cables, sometimes inner high (masts) or low points and sometimes inner ridge and valley cables. By varying the geometry of the boundary or inner supports, architect or structural engineer can influence the form of the fabric structure.

J. Dvornik and D. Lazarević initiated development of an interactive computer program that will help architects and structural engineers in designing tensile structures [5]. Design of tensile structures can be divided into three phases: definition of the form of the structure loaded only with prestressing forces (form finding), analysis of structure's behaviour under varying loads, and definition of the cutting patterns of the fabric. In this article we describe one approach to the first phase.

J. Douglas wrote in [4]: "The spirit of this paper being entirely numerical, we do not concern ourselves with theoretical questions of convergence, which are besides too difficult for us to deal with. Whether convergence occurs or not is indicated practically in each particular case by the behavior of the numbers obtained in the course of the computation." These words can be taken as a motto of the present paper.

2. Minimal surface problem

As already said, structural fabric has very low shear and no compressive stiffness. Therefore, to avoid wrinkles caused by compressive or shear stresses, it is highly desirable to establish a uniform state of tensile (pre)stress in the fabric structure: throughout the surface and, at each point, in all directions of the tangential plane, tensile stresses should be (approximately) equal. (With pretension high enough, we can neglect the weight of the fabric.) In isostress state fabric membrane will behave essentially like a soap film, and the form finding problem can be reduced to the well known minimal surface or Plateau's problem.

We will describe here the so-called restricted, or nonparametric, form of the minimal surface problem which suffices for most structural applications when the boundary consists of rigid beams or arcs.

Suppose that the system of straight or curved supporting beams can be described by a non-self-intersecting, closed, piecewise smooth curve k in $\mathbb{R}^3$, whose orthogonal projection onto the (x, y)–plane is a boundary $\partial\Omega$ of a simply connected domain Ω. Curve k can be defined as a graph of some function $g : \partial\Omega \to \mathbb{R}$.

Let σ be the soap film tension; under certain conditions it is independent of the area of the soap film [10]. The energy of the soap film is therefore proportional to the surface area. Since energy is minimized when the film is in stable equilibrium, equilibrium configuration is the configuration with the least possible area. Hence, the problem is to find the function $u : \Omega \to \mathbb{R}$ which minimizes area functional

$$F[u] = \iint_{\Omega} \sqrt{1 + (\partial_x u)^2 + (\partial_y u)^2}\, dx\, dy \tag{1}$$

and satisfies boundary condition

$$u(x, y) = g(x, y) \quad \text{on } \partial\Omega.$$

The condition for a minimum of $F[u]$ is

$$\frac{\partial}{\partial x}\left(\frac{\partial_x u}{\sqrt{1 + (\partial_x u)^2 + (\partial_y y)^2}}\right) + \frac{\partial}{\partial y}\left(\frac{\partial_y u}{\sqrt{1 + (\partial_x u)^2 + (\partial_y y)^2}}\right) = 0, \tag{2}$$

which, after differentiation and some simple manipulations, gives

$$\left[1 + (\partial_y u)^2\right] \partial_{xx} u - 2\, \partial_x u\, \partial_y u\, \partial_{xy} u + \left[1 + (\partial_x u)^2\right] \partial_{yy} u = 0. \tag{3}$$

If the surface is shallow, then $\partial_x u \ll 1$ and $\partial_y u \ll 1$ and equation (3) can be approximated by Laplace equation

$$\Delta u = \partial_{xx} u + \partial_{yy} u = 0. \tag{4}$$

3. Finite difference discretizations

The first method for the numerical solution of the minimal surface equation was proposed in 1928 by J. Douglas [4]: by using a nine-point difference star he derived a system of nonlinear algebraic equations[1].

By approximating partial derivatives $\partial_x u$ and $\partial_y u$ in surface area functional (1) alternately by forward and backward differences and applying the conditions for a minimum of discretized functional, D. Greenspan obtained first order accurate difference equations [7].

P. Concus modified his previously developed scheme for the numerical solution of the two-dimensional nonlinear magnetostatic field equation and developed finite difference equations that approximate differential equation (2) at interior points (ih, jh) of the finite difference mesh with second order accuracy [3].

By approximating $\partial_x u$ and $\partial_y u$ in $F[u]$ at auxiliary points $\left((i + \frac{1}{2})h, (j + \frac{1}{2})h\right)$ by central differences, T. Meis derived similar, though simpler, difference equations [11].

[1] In 1931 Douglas proved the existence of the solution to the Plateau's problem for disk-type surfaces. Another proof was given in 1930 by T. Rado.

Systems of nonlinear difference equations were iteratively solved in [3, 7, 11] by one-step successive overrelaxation–Newton (SOR–Newton) method:

$$u_i^{(k)} = u_i^{(k-1)} - \omega \cdot \frac{f_i\big(u_1^{(k)}, \ldots, u_{i-1}^{(k)}, u_i^{(k-1)}, u_{i+1}^{(k-1)}, \ldots, u_n^{(k-1)}\big)}{\frac{\partial f_i}{\partial u_i}\big(u_1^{(k)}, \ldots, u_{i-1}^{(k)}, u_i^{(k-1)}, u_{i+1}^{(k-1)}, \ldots, u_n^{(k-1)}\big)}, \tag{5}$$

while in [13] D. O'Leary analysed and compared several variants of (preconditioned) nonlinear conjugate gradient algorithms applied to Concus' equations.

4. Finite element discretization

For practical, engineering applications, finite element method is of wider applicability than finite difference method. Finite difference discretizations are usually confined to rectangular domains as the approximation near the boundary of an irregular domain may be less accurate than in the interior. To restore accuracy, some special tricks (e.g., higher order discretization) are needed. Finite elements more readily, with equal accuracy on uniform and nonuniform meshes, adapt to complex, irregular domains.

We approximate the closure $\overline{\Omega}$ of the given domain Ω by admissible, shape regular triangulation $\mathcal{T}^h = \bigcup_{i=1}^{t} T_i$, where h is the "mesh size": $h = \max_{T_i} \operatorname{diam} T_i$.

Set $\mathcal{N}^h$ of all n vertices N_k in $\mathcal{T}^h$ can be divided into two disjoint subsets: the set $\mathcal{N}_{\mathrm{I}}^h$ of n_{I} interior vertices and the set $\mathcal{N}_{\mathrm{B}}^h$ of n_{B} vertices that lie on $\partial\Omega$.

Let $\mathcal{S}^h$ be the linear space of continuous, piecewise linear functions defined on $\mathcal{T}^h$: $\mathcal{S}^h = \big\{v \in C^0(\mathcal{T}^h) \mid \bar{v}_i \text{ linear}\big\}$, where $\bar{v}_i = v|_{T_i}$; let $\mathcal{S}_0^h \subset \mathcal{S}^h$ be the linear space of functions in $\mathcal{S}^h$ which are zero on the vertices in $\mathcal{N}_{\mathrm{B}}^h$ and let $\mathcal{S}_g^h \subset \mathcal{S}^h$ be the affine space of functions in $\mathcal{S}^h$ which assume the same values as g on the vertices in $\mathcal{N}_{\mathrm{B}}^h$.

Function $v \in \mathcal{S}^h$ can be written as a linear combination of the nodal basis functions φ_k^h, where coefficients (denoted here by u_k) are the values of the function v on the vertices $N_k \in \mathcal{N}^h$. Functional $F[v]$ can thus be transformed into function of n variables u_k (or, shorter, of vector variable $\mathbf{u} \in \mathbb{R}^n$):

$$F(u_1, \ldots, u_n) = F(\mathbf{u}) = \sum_{T_i \in \mathcal{T}} \iint_{T_i} \sqrt{1 + (\partial_x \bar{v}_i)^2 + (\partial_y \bar{v}_i)^2}\, dx\, dy,$$

and, if we denote the area of triangle T_i by $A(T_i)$:

$$F(\mathbf{u}) = \sum_{T_i \in \mathcal{T}} A(T_i) \sqrt{1 + (\partial_x \bar{v}_i)^2 + (\partial_y \bar{v}_i)^2}. \tag{6}$$

Conditions for a minimum of the function $F(\mathbf{u})$, that is, for a minimal approximate area, lead to the system of n_{I} algebraic equations

$$f_k(\mathbf{u}) = \frac{\partial \mathcal{F}(\mathbf{u})}{\partial u_k} = \frac{1}{2} \sum_{T_i \ni N_k} \frac{\alpha_{i_k}\, \partial_x \bar{v}_i + \beta_{i_k}\, \partial_y \bar{v}_i}{\sqrt{1 + (\partial_x \bar{v}_i)^2 + (\partial_y \bar{v}_i)^2}} = 0, \tag{7}$$

where k is such that $N_k \in \mathcal{N}_{\mathrm{I}}^h$, while $\alpha_{i_k} = y_{i_{\mathrm{ccw}}} - y_{i_{\mathrm{cw}}}$ and $\beta_{i_k} = x_{i_{\mathrm{cw}}} - x_{i_{\mathrm{ccw}}}$, with indices 'cw' and 'ccw' denoting vertices that lie clockwise and counter-clockwise with respect to the vertex N_k in the triangle T_i. This system is supplemented with n_{B} discretized boundary conditions for nodes $N_k \in \mathcal{N}_{\mathrm{B}}^h$.

The first application of finite element method to minimal surface problem was described in [9]. Hinata et al. pointed out that it is not necessary to fix the triangulation of Ω, but only to minimize functional (6) and that, therefore, nodes may be treated as unknown points in $\mathbb{R}^3$. That observation enabled them to solve a free boundary form of Plateau's problem. H.–J. Wagner devised an approximation of parametric minimal surfaces [15]. As a direction in which unknown point P_i in $\mathbb{R}^3$ could be varied in the minimization process he proposed the resultant of vectors normal to the triangles with vertex P_i. Nonlinear algebraic systems resulting from discretization were in both papers solved by SOR–Newton method (5). H. Mittelmann proposed a modified relaxation scheme less dependent on correct choice of ω, accelerated with conjugate gradients [12].

In [9, 15] discretization and solution methods were described and verified on several numerical examples, but no convergence proofs were given. H. Mittelmann gave several error estimates for approximations of minimal and capillary surfaces with linear finite elements and a convergence proof for modified relaxation method, see [12] and references therein.

5. Multigrid method

The basic "multigrid philosophy" was stated by A. Brandt in his fundamental paper [2]: "... the algebraic system to be solved does not stand by itself, but is actually an approximation to continuous equations, and therefore can itself be similarly approximated by other (much simpler) algebraic systems." This relation between discretizations of a differential or a variational equation on grids of different coarseness can be used in two related ways: as a multigrid cycle and as a nested iteration.

For nonlinear systems it is crucial to start iteration with a good initial guess; otherwise, the process (not only multigrid, but other "classical" methods as well) may diverge. Simple and obvious way of obtaining first approximation of the solution on a given grid was devised long ago: in those old days when computers were (groups of) people, common approach was to approximately solve the problem on an auxiliary grid with about one tenth of the final number of nodes, and then to interpolate the solution onto the finer grid [14]. Immediate generalization is to introduce several progressively finer grids. When the (approximate) solution on each level, except on the coarsest one, is computed by multigrid algorithm, method is called full multigrid or, more often, picturesquely: nested iteration.

Another procedure that strongly influenced the development of multigrid method was also described in Southwell's book [14]: "block" and, more generally, "group relaxation" in which several nodes were simultaneously relaxed, "the aim being to reduce

the total energy by as great an amount as possible". But, those techniques were derived from and for specific engineering problems and were tailored for "hand" calculations (e.g., in each step nodes with greatest residual were relaxed); therefore, they were unsuitable for development of abstract algorithms that can be mechanically executed. It is considered that the origin of the modern multigrid method(s) was A. Brandt's paper [2] in which the precise descriptions of linear (CS) and nonlinear (FAS) algorithms were given[2]. Brandt's starting point was the observation that "classical" relaxation schemes, like linear or nonlinear Gauß–Seidel sweeps, rapidly decrease the residual as long as it strongly oscillates on the scale of the grid. In the multigrid cycle, therefore, relaxation on the given grid is used to reduce the high-frequency components of the residual, while the lower frequencies are reduced on coarser grids where they again appear oscillatory.

Thus, both for nested iteration and for multigrid cycle, we need a hierarchy of increasingly finer grids. In finite difference method we construct consecutive meshes with steps $h, h/2, h/4, \ldots, h/2^m$, while the simplest way to construct the hierarchy of finite element triangulations is to subdivide each triangle in coarser triangulation $\mathcal{T}^{h_\ell}$ into four congruent triangles by bisecting its edges, which results in a triangulation $\mathcal{T}^{h_{\ell+1}}$. Let $\mathcal{S}_\ell$ be the finite element space associated with the triangulation $\mathcal{T}^{h_\ell}$; then $\mathcal{S}_\ell \subset \mathcal{S}_{\ell+1}$. If the boundary $\partial\Omega$ is curved, new vertices on level $\ell+1$, which would otherwise lie at the midpoints of the level ℓ edges with two vertices on $\partial\Omega$, can be "moved" to the boundary. Shapes of the triangles near the boundary are then distorted, and the inclusion $\mathcal{S}_\ell \subset \mathcal{S}_{\ell+1}$ is violated there, but it still holds for most of the elements.

We can write system (7), or a similar system of difference equations (sec. 3), in shorter form as $\mathbf{F}_\ell(\mathbf{u}_\ell) = \mathbf{0}_\ell$, where nonlinear operator $\mathbf{F}_\ell : \mathbb{R}^{n_\ell} \to \mathbb{R}^{n_\ell}$ results from discretization on the mesh on level ℓ. In the course of the multigrid cycle some additional (constant) terms are generated on all levels except the highest, see eq. (9); the previous equation should, therefore, be generalized to

$$\mathbf{F}_\ell(\mathbf{u}_\ell) = \mathbf{b}_\ell, \qquad \mathbf{F}_\ell : \mathbb{R}^{n_\ell} \to \mathbb{R}^{n_\ell}, \tag{8}$$

with $\mathbf{b}_m = \mathbf{0}_m$ on the finest mesh (level m).

For a transfer between levels we will need two (linear) operators: a projection operator $\mathbf{I}_\ell^{\ell-1} : \mathbb{R}^{n_\ell} \to \mathbb{R}^{n_{\ell-1}}$ and an interpolation operator $\mathbf{I}_{\ell-1}^{\ell} : \mathbb{R}^{n_{\ell-1}} \to \mathbb{R}^{n_\ell}$. In finite element setting, canonical interpolation and projection operators are frequently used. Let $\mathbf{u}_{\ell-1} \in \mathbb{R}^{n_{\ell-1}}$ and $\mathbf{u}_\ell \in \mathbb{R}^{n_\ell}$ be the coefficient vectors of $v \in \mathcal{S}_{\ell-1}$ and $\bar{v} \in \mathcal{S}_\ell$, respectively. We set $\bar{v} = v$ using the inclusion $\mathcal{S}_{\ell-1} \subset \mathcal{S}_\ell$. Requirement that $\mathbf{I}_{\ell-1}^{\ell}\mathbf{u}_{\ell-1}$ be the coefficient vector of $\bar{v} = v$ with respect to the basis of $\mathcal{S}_\ell$ defines canonical interpolation operator $\mathbf{I}_{\ell-1}^{\ell}$ (for linear finite elements this is linear interpolation). Canonical projection operator is then defined by $\mathbf{I}_\ell^{\ell-1} = c(\mathbf{I}_{\ell-1}^{\ell})^{\mathrm{T}}$, where constant c

[2]Independently, W. Hackbusch discovered multigrid procedure in 1976. His nonlinear multigrid algorithm [8] is a generalization of Brand's FAS.

depends on "mesh sizes" h_ℓ and $h_{\ell-1}$. Straight injection, where v and $\bar{v}$ have the same values on common vertices, can also be used for projection.

Let the symbol $\tilde{\mathbf{u}}_\ell$ denote some approximate solution to the system (8). The residual is defined by

$$\mathbf{r}_\ell = \mathbf{b}_\ell - \mathbf{F}_\ell(\tilde{\mathbf{u}}_\ell),$$

and, since $\mathbf{F}_\ell(\mathbf{u}^*_\ell) \equiv \mathbf{b}_\ell$ for the (exact) solution $\mathbf{u}^*_\ell$, this equation can be written as

$$\mathbf{F}_\ell(\mathbf{u}^*_\ell) - \mathbf{F}_\ell(\tilde{\mathbf{u}}_\ell) = \mathbf{r}_\ell.$$

If fluctuating components of the residual $\mathbf{r}_\ell$ are damped by the so-called presmoothing relaxation sweeps, we can write an approximation on the lower level:

$$\mathbf{F}_{\ell-1}(\mathbf{u}_{\ell-1}) - \mathbf{F}_{\ell-1}(\mathbf{I}^{\ell-1}_\ell \tilde{\mathbf{u}}_\ell) = \mathbf{I}^{\ell-1}_\ell \mathbf{r}_\ell;$$

here we treat $\mathbf{u}_{\ell-1}$ as the unknown. If we introduce the notation

$$\mathbf{b}_{\ell-1} = \mathbf{F}_{\ell-1}(\mathbf{I}^{\ell-1}_\ell \tilde{\mathbf{u}}_\ell) + \mathbf{I}^{\ell-1}_\ell \mathbf{r}_\ell, \tag{9}$$

the previous equation becomes

$$\mathbf{F}_{\ell-1}(\mathbf{u}_{\ell-1}) = \mathbf{b}_{\ell-1}, \qquad \mathbf{F}_{\ell-1} : \mathbb{R}^{n_{\ell-1}} \to \mathbb{R}^{n_{\ell-1}}, \tag{10}$$

and this equation is of the same form as the equation (8). Let $\mathbf{u}^*_{\ell-1}$ be the solution to the equation (10); we can interpolate it back to the level ℓ to correct the previous approximate solution:

$$\tilde{\tilde{\mathbf{u}}}_\ell = \tilde{\mathbf{u}}_\ell + \mathbf{I}^\ell_{\ell-1}(\mathbf{u}^*_{\ell-1} - \mathbf{I}^{\ell-1}_\ell \tilde{\mathbf{u}}_\ell).$$

This new approximation can be improved by further, the so-called postsmoothing, relaxation sweeps.

One important observation is that each $\tilde{\mathbf{u}}_\ell$ is the projection of the (approximate) solution $\tilde{\mathbf{u}}_m$ on the finest mesh, $\tilde{\mathbf{u}}_\ell = \mathbf{I}^\ell_m \tilde{\mathbf{u}}_m$. This scheme is, therefore, called the full approximation storage (FAS) algorithm[3]. Various orders of visiting consecutive levels are called V-, W-, sawtooth-, etc., multigrid cycles.

6. Numerical results

We tuned and tested our multigrid computer program on Concus' and Meis' finite difference discretizations[4] and on finite element discretization (7). Results of numerical experiments with Concus' equations on square domain were described in [6]; Meis'

[3]In linear version, systems $\mathbf{A}_\ell \mathbf{e}_\ell = \mathbf{r}_\ell$, where $\mathbf{e}_\ell$ is the error, are solved on coarser grids; therefore, linear version is called the correction storage (CS) algorithm.

[4]Unrelated to the minimal surface problem, we also tested our program on FD discretizations of linear Laplace and nonlinear Bratu's differential equations, because precise numerical data can be found in literature about the behaviour of some MG programs when applied to them.

equations gave similar results. Here we will mention some examples and applications of finite element discretization.

One test example was Scherk's minimal surface

$$u(x, y) = \ln(\cos x / \cos y).$$

This surface is suitable for thorough numerical testing and for tuning of various parameters of (abstract) multigrid algorithm to get robust and efficient solver, because, depending on the choice of $\overline{\Omega}$, it can exhibit well-behaved or pathological behaviour. It is defined (that is, real-valued) on the set $\{(u, v) \mid \cos u \cos v > 0\}$, for example, on the square $\left(-\frac{\pi}{2}, \frac{\pi}{2}\right)^2$. Planes $x = \pm\frac{\pi}{2}$ and $y = \pm\frac{\pi}{2}$ are asymptotic planes and surface steeply tends to $\pm\infty$ while approaching them.

For pre- and postsmoothing sweeps one-step Gauß–Seidel–Newton algorithm, i.e., (5) with $\omega = 1$, was chosen. Overrelaxation ($\omega > 1$) didn't accelerate convergence rate significantly and sometimes led to divergence. It seems that the optimal number of pre- and postsmoothing sweeps for our problem is four to six.

Coarse finite element mesh, which is used both as an initial mesh in nested iteration and as a lowest level in multigrid cycle, must be (in current version of the program) manually defined. Initial approximation is the solution of the Laplace equation (4) with the same boundary conditions, because it was observed that for arbitrary first approximation (e.g., common choice $\mathbf{u}_0 = \mathbf{0}$) nonlinear iteration sometimes, specially when boundary conditions were not in some sense symmetric, diverged even on the very coarse grid. (We also experimented with nonlinear underrelaxation, i.e., $\omega < 1$ in (5), but it seems that the proper choice of ω depends on the concrete form of the boundary and, therefore, it is difficult to propose a robust algorithm.)

As the stopping criterion for the multigrid iteration on level ℓ we use

$$\|\mathbf{r}_\ell\| \leq 0.1 \, \|\boldsymbol{\tau}_\ell^{\ell-1}\|,$$

where

$$\boldsymbol{\tau}_\ell^{\ell-1} = \mathbf{F}_{\ell-1}(\mathbf{I}_\ell^{\ell-1}\mathbf{u}_\ell^*) - \mathbf{I}_\ell^{\ell-1}\mathbf{F}_\ell\mathbf{u}_\ell^* = \mathbf{b}_{\ell-1} - \mathbf{I}_\ell^{\ell-1}\mathbf{b}_\ell$$

is the relative (local) truncation error.

Convergence history for Scherk's surface on $\overline{\Omega} = [-1, 1]^2$ is shown in Table 1, where $\mathbf{r}_\ell^{(k)}$ denotes residual on level ℓ after k-th cycle and $\varepsilon = \|\mathbf{r}_\ell^{(k)}\|_\infty / \|\mathbf{r}_\ell^{(k-1)}\|_\infty$. Domain was divided into regular mesh with 32 triangles and 25 nodes, 9 of which were interior. Mesh on level 3 had 2048 elements, 833 interior and 128 boundary nodes. As can be seen from Table 1, on the finest mesh 5 multigrid cycles were needed to satisfy the given convergence criterion. In Table 2, numbers of cycles needed for convergence on the third level are shown for different choices of $\overline{\Omega}$. Triangulations were as in the first example.

Similar results were obtained on hexagonal and irregular polygonal domains, and on domains with curved boundaries which were defined as cubic splines with chord-length parametrization.

ℓ	k	$\|\mathbf{r}_\ell^{(k)}\|_\infty$	ε
0	–	$1.72390 \cdot 10^{-15}$	–
1	1	$6.97805 \cdot 10^{-4}$	–
	2	$1.48455 \cdot 10^{-4}$	0.212746
2	1	$3.86230 \cdot 10^{-4}$	–
	2	$6.82710 \cdot 10^{-5}$	0.176762
	3	$2.09598 \cdot 10^{-5}$	0.307009
3	1	$1.10594 \cdot 10^{-4}$	–
	2	$2.57059 \cdot 10^{-5}$	0.232435
	3	$1.10082 \cdot 10^{-5}$	0.428236
	4	$5.13117 \cdot 10^{-6}$	0.466123
	5	$2.72290 \cdot 10^{-6}$	0.530659

Table 1.

$\overline{\Omega}$	$k_{\max}$	$\|\mathbf{r}_3^{(k_{\max})}\|_\infty$
$[-1.2, 1.2] \times [-1.2, 1.2]$	5	$1.00602 \cdot 10^{-5}$
$[-1.4, 1.4] \times [-1.4, 1.4]$	5	$7.81262 \cdot 10^{-5}$
$[-1.5, 1.5] \times [-1.5, 1.5]$	7	$1.98717 \cdot 10^{-4}$
$[0, 1] \times [0, 1]$	7	$1.57329 \cdot 10^{-7}$
$[0, 1.2] \times [0, 1.2]$	6	$8.26654 \cdot 10^{-7}$
$[0, 1.5] \times [0, 1.5]$	8	$3.10647 \cdot 10^{-5}$
$[-0.6, 0.6] \times [0, 1.2]$	8	$8.67581 \cdot 10^{-7}$

Table 2.

As a final example we show one practical application. Architect A. Kuzmanić proposed fabric roofs for the new bus terminal at Dubrovnik airport. J. Dvornik and D. Lazarević made the preliminary design. Each roof will be assembled of six modules. Three modules are depicted in Figure 1, with the other three being mirror images (bounding-box side on the right is the plane of symmetry).

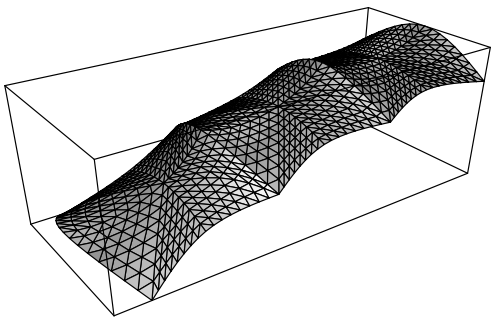

Figure 1.

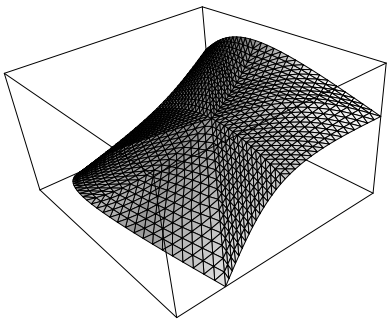

Figure 2.

Two edges of each module are rigid arcs, while the other two are flexible cables; adjacent modules share a common arc and cables run along the longer sides of the roof. Rigid arcs are inclined parabolic arcs. Flexible edges, whose shape can't be determined *a priori*, but through the same form finding process, are not included in the current version of our program. Their shape is, therefore, determined approximately by the procedure described in [1]. Cubic spline is interpolated through the calculated discrete points so that the nodes of refined finite element meshes can be placed on the boundary.

The roof surface of each module will be the minimal surface spanned between the previously defined boundary curves.

Initial, manually created mesh (level 0) for each module had 9 nodes, with only 1 interior node, and 8 triangles. Meshes were refined up to the fifth level, with 4225 nodes (3969 interior nodes, i.e., unknowns) and 8192 elements. In Figure 1, meshes on the third level are shown and Figure 2 depicts the mesh of the leftmost module on the fourth level.

Because all three surfaces are relatively shallow, convergence was rather fast. On levels 1 and 2 in each case only one multigrid cycle was needed to satisfy the given criterion, while on levels 3, 4 and 5 two cycles were needed. Norms of the residuals on the fourth level were $\mathbf{r}_4^{(2)} \approx 1 \cdot 10^{-4}$ and on the fifth level $\mathbf{r}_5^{(2)} \approx 2.5 \cdot 10^{-5}$.

References

[1] H. Berger, *Light Structures, Structures of Light. The Art and Engineering of Tensile Architecture*, Birkhäuser, Basel, 1996.

[2] A. Brandt, *Multi-level adaptive solutions to boundary-value problems*, Math. Comp., 31 (1977), pp. 333–390.

[3] P. Concus, *Numerical solution of the minimal surface equation*, Math. Comp., 21 (1967), pp. 340–350.

[4] J. Douglas, *A method of numerical solution of the problem of Plateau*, Ann. of Math., 2 (1928), pp. 180–188.

[5] J. Dvornik i D. Lazarević, *Viseće konstrukcije od platna i užadi*, Građevni godišnjak '97, HDGI, Zagreb, 1997, pp. 239–297.

[6] K. Fresl, *Primjena višerazinske metode u oblikovanju konstrukcija od platna*, Građevinar, 49 (1997), pp. 537–549.

[7] D. Greenspan, *Lectures on the Numerical Solution of Linear, Singular, and Nonlinear Differential Equations*, Prentice–Hall, Englewood Cliffs, NJ, 1968.

[8] W. Hackbusch, *Multi–Grid Methods and Applications*, Springer–Verlag, Berlin, New York, 1985.

[9] M. Hinata, M. Shimasaki, and T. Kiyono, *Numerical solution of Plateau's problem by a finite element method*, Math. Comp., 28 (1974), pp. 45–60.

[10] C. Isenberg, *The Science of Soap Films and Soap Bubbles*, Dover, New York, 1992.

[11] T. Meis, *Zur Diskretisierung nichtlinearer elliptischer Differentialgleichungen*, Computing, 7 (1971), pp. 344–352.

[12] H. D. Mittelmann, *On the efficient solution of nonlinear finite element equations I*, Numer. Math., 35 (1980), pp. 277–291.

[13] D. P. O'Leary, *Conjugate gradient algorithms in the solution of optimization problems for nonlinear elliptic partial differential equations*, Computing, 22 (1979), pp. 59–77.

[14] R. V. Southwell, *Relaxation Methods in Engineering Science*, Oxford University Press, London, 1940.

[15] H.–J. Wagner, *A contribution to the numerical approximation of minimal surfaces*, Computing, 19 (1977), pp. 35–58.